Polymer 49 (2008) 4446–4455

Contents lists available at ScienceDirect

Polymer

journal homepage: www.elsevier.com/locate/polymer

Effect of chemical structure and crosslinking density on the thermo-mechanical properties and toughness of (meth)acrylate shape memory polymer networks

David L. Safranski [a,*], Ken Gall [a,b]

[a] School of Materials Science and Engineering, Georgia Institute of Technology, 771 Ferst Dr, Love Manufacturing Building Atlanta, GA 30332, United States
[b] Woodruff School of Mechanical Engineering, Georgia Institute of Technology, Atlanta, GA 30332, United States

ARTICLE INFO

Article history:
Received 4 May 2008
Received in revised form 17 July 2008
Accepted 26 July 2008
Available online 7 August 2008

Keywords:
(Meth)acrylate networks
Mechanical properties
Toughness

ABSTRACT

The objective of this work is to characterize and understand structure–mechanical property relationships in (meth)acrylate networks. The networks are synthesized from mono-functional (meth)acrylates with systematically varying sidegroup structure and multi-functional crosslinkers with varying mole fraction and functionality. Fundamental trends are established between the network chemical structure, crosslink density, glass transition temperature, rubbery modulus, failure strain, and toughness. The glass transition temperature of the networks ranged from −29 to 112 °C, and the rubbery modulus (E_r) ranged from 2.8 to 129.5 MPa. At low crosslink density ($E_r < 10$ MPa) network chemistry has a profound effect on network toughness. At high crosslink densities ($E_r > 10$ MPa), network chemistry has little influence on material toughness. The characteristic ratio of the mono-functional (meth)acrylates' components is unable to predict trends in network toughness as a function of chemical structure, as has been demonstrated in thermoplastics. The cohesive energy density is a better tool for relative prediction of network mechanical properties. Due to superior mechanical properties, networks with phenyl sidegroups are further investigated to understand the effect of phenyl sidegroup structure on toughness.

1. Introduction

The shape memory effect in polymers has been used in engineering applications since 1960s, when radiation crosslinked polyethylene was employed for heat shrink tubing. More recently, researchers have focused on biomedical applications of shape memory polymers. Novel cardiac devices have been proposed as actuators for stroke victims and self-deploying stents for treatment of arterial disease [1,2]. Other shape memory polymers have been used for neuronal probes [3]. While shape memory polymers may vary in chemical composition, method of activation, and mode of degradation, their ability to change and maintain distinct shapes is pivotal. The broad range of applications gives rise to a diverse set of required polymer property requirements in shape memory polymers. For example, it is well known that the glass transition temperature controls activation time and temperature while the rubbery modulus controls activation force level. However, little work has been performed to understand strain to failure in shape memory polymer networks and the corresponding toughness, which governs the available work capacity in the materials.

The structure of (meth)acrylate networks formed through free radical polymerization has been studied by kinetic models and experimental research [4–8]. The network backbones are primarily carbon–carbon bonds formed by free radical polymerization with remaining backbones defined by finite length crosslinking monomers. The relationships between the reactivity of the double bond functional group and monomer size, fraction of monomer, conversion, free volume, and initiation have been studied as well [7]. Differences between multi-functional acrylates and methacrylates have been studied. The multi-functional acrylates polymerize three to seven times faster than their corresponding methacrylates, including a more uniform polymerization, but at the sacrifice of lower strength and more volume shrinkage [9–11]. There are polymerization differences between di-functional monomers and monomers of greater functionality, where di-functional monomers are more reactive due to lower viscosities driven by lower individual molecular weight [8]. Effects of temperature, light intensity, and concentration have been studied in thicker films where heat and mass transfer were considered. The larger size samples retained heat, thus allowing for greater conversion approaching unity [12]. The thermo-mechanical properties and polymerization rate decrease as the kinetic chain length decreases, but the effect diminishes as the crosslinking density increases [13]. A relationship affecting structural heterogeneity has been observed where increasing the crosslink density increases the heterogeneity of the

* Corresponding author. Tel.: +1 404 385 0624; fax: +1 404 894 9140.
E-mail address: safranski@gatech.edu (D.L. Safranski).

0032-3861/$ – see front matter © 2008 Elsevier Ltd. All rights reserved.
doi:10.1016/j.polymer.2008.07.060

polymer for blends of mono-functional and multi-functional (meth)acrylates [5]. From these studies, the polymerization kinetics have provided the fundamental relationships between network structure and processing conditions.

The tailorability of the thermo-mechanical properties of (meth)acrylate networks as shape memory polymers has previously been established. The glass transition temperature (T_g) and rubbery modulus can be varied independently of each other, where T_g primarily controls the free strain recovery time and E_r primarily controls the constrained recovery force [14]. Also, the effect of crosslinker concentration on E_r has been determined in (meth)acrylate networks; increasing the amount of crosslinker increases the E_r [15]. These qualities allow for various biomedical applications with a wide array of mechanical property requirements. However, the total shape change (strain) possible in these systems has not been fully explored. It is known that if heated above the compositions' T_g, (meth)acrylate networks will fully recover strains near to their failure strain due to the chemical crosslinking [16]. As such, many thermosets have a strain recovery ratio approaching 100% [17].

Given the high strain recovery ratio in thermosets, the failure strain of the network is the limiting factor in shape recoverability. Prior work had demonstrated that as the crosslink density increases, the ultimate strength increases and the failure strain decreases [18]. A region of insensitivity to failure strain was discovered at high crosslink densities for an acrylate system, and the failure mechanisms differed in regions of low and high crosslink densities [19]. After accounting for crosslinking effectiveness through rubbery modulus, the choice of crosslinker does not drastically change the failure strain in networks formed from mono-functional and di-functional (meth)acrylates [18]. In summary, although failure strain and rubbery modulus will be naturally traded off in a network as a function of changing crosslink density, the role of network chemistry on toughness (large strain capacity at equivalent rubbery modulus) in (meth)acrylates is relatively unexplored.

The large strain capacity and toughness of polymers have been studied extensively in thermoplastic materials. The characteristic ratio (C_∞), first suggested by Flory [20], describes the ability of a polymer chain to coil. A series of studies has described the theoretical prediction of C_∞ based upon chemical structure, and trends between C_∞ and mechanical properties [21–24]. C_∞ is calculated by using group contributions from the intrinsic viscosity of the polymer, which fall within 7% of the experimental outcomes. C_∞ can be used to define the brittle–ductile transition temperature in many thermoplastics, where polymers with C_∞ values less than 7.5 typically fail by yielding, and polymers with C_∞ values above 7.5 typically fail by crazing. When $C_\infty = 1$, the polymer has a random walk structure, and ideal tetrahedral skeletal bonds along the backbone chain have a $C_\infty = 2$. Thus, as the C_∞ of the polymer approaches 2, the polymer becomes intrinsically more ductile, such as polycarbonate, which has $C_\infty = 2.4$. The lowest (meth)acrylate is methyl acrylate at 7.5, which falls on the border of yielding and crazing for a thermoplastic material. The characteristic ratio does not take into account the effect of crosslinking, and the limit of applying this parameter to networks has yet to be determined.

Another parameter used to predict chemical and mechanical properties of polymers is the cohesive energy density (CED), which characterizes the intermolecular interactions in polymers. The CED can be determined by calculation through group contributions, swelling experiments, bulk modulus measurements, and modeling methods [25–31]. The preferred methods of determination are the characterization of bulk modulus at low temperatures or high frequencies and calculation by group contributions. Swelling is not the preferred method of characterization because of the ambiguity associated with the methodology [32]. The CED has become a widely used parameter to predict properties such as elastic modulus, surface tension, and yield stress [26,27,33]. Recent modeling has shown that as the crosslink density of an epoxy network decreases, the CED increases [34]. Thus as the crosslinking density decreases, the linear monomer backbone structures exert increasing influence. At present, the influence of systematically varying cohesive energy density and crosslinking density on the mechanical properties of (meth)acrylate networks is unknown.

The purpose of this study will be to determine the effect of chemical structure and crosslinking density on both the thermal and mechanical properties of (meth)acrylate networks. The effect of chemical structure on thermal properties will be revealed through systematic variation of a diverse set of monomers. A series of networks with the same crosslinker and varying mono-functional monomer will be studied in order to assess the influence of the mono-functional monomer on the networks' properties. Emphasis will be placed on failure strain and material toughness due to the importance of these properties in shape change and actuation capacity in shape memory polymers. Basic parameters, C_∞ and CED are used to help interpret chemical influences on the mechanical properties of the networks.

2. Experimental

2.1. Materials

Sixteen mono-functional (meth)acrylates were used as the linear chain builders and 16 multi-functional (meth)acrylates were used as the crosslinkers to form the polymer networks. The names, abbreviations, chemical structures, and molecular weights can be found in Charts 1 and 2. A set of networks comprised of 10 mole percent (mol%) PEGDMA550 were copolymerized with each mono-functional acrylate from Chart 1. A set of networks comprised of 10 mol% of each crosslinker from Chart 2 were copolymerized with 90 mol% tBA. These sets were calculated using the molecular weights given in Charts 1 and 2. In addition, equivalent molar amounts of BMA, tBA, and EEM were copolymerized in varying degrees with PEGDMA550. The mol% and corresponding weight percent (wt%) ratios of these three sets of materials can be found in Table S1. The photoinitiator, 2,2-dimethoxy-2-phenylacetophenone, was added to each material in an amount of 0.5 wt%. Further equivalent molar amounts of BZA and EGPEM were copolymerized with PEGDMA550, which can be found in Table S2. Ternary polymer networks with a fixed 2.5 mol% PEGDMA550 are described in Table S3. All materials were purchased from Sigma Aldrich or Polysciences and used as received.

2.2. Methods

The polymer solutions were injected into a mold composed of two glass slides separated by 1 mm spacers. Glass slides were cleaned with Alconox then coated with Rain-X as a mold release agent. The injected molds were polymerized under a 365 nm UV lamp for an average of 20 min, while materials with low concentrations of crosslinker could take over 30 min. For each material set in Tables S1–S3, two batches of each composition were created separately.

Samples for dynamic mechanical analysis (DMA) were prepared by laser cutting specimens to 20 mm × 5 mm × 1 mm from bulk material. A TA Q800 was used in tensile loading with strain of 0.2%, preload of 0.001 N, force track of 150%, and frequency of 1 Hz. The samples were equilibrated at −50 °C for 2 min then raised to 200 °C at a rate of 5 °C/min ($n \geq 2$). The glass transition temperature was defined as the peak of the tan δ curve from the DMA testing.

Mechanical tensile testing was performed on dogbones of half size ASTM D638 type IV, which was laser cut from 1 mm thick

Chart 1

Monomer	Structure	Molecular weight (g/mol)
Methyl acrylate (MA)	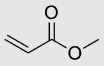	86.09
Methyl methacrylate (MMA)	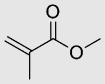	100.12
Butyl acrylate (BA)	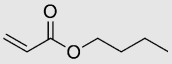	128.17
tert-Butyl acrylate (tBA)	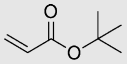	128.17
tert-Butyl methacrylate (tBMA)	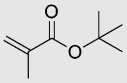	142.20
2-Ethoxyethyl methacrylate (EEM)	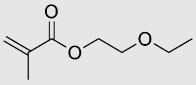	158.19
Isobornyl methacrylate (IMA)	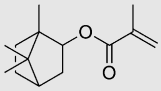	222.32
2-Ethylhexyl methacrylate (2EHM)	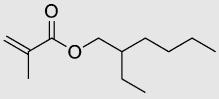	198.3
Isodecyl acrylate (IA)	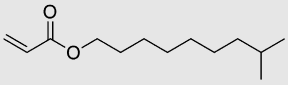	212.33
Benzyl methacrylate (BMA)	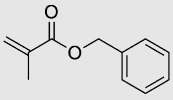	176.21
Ethylene glycol phenyl ether methacrylate (EGPEM)	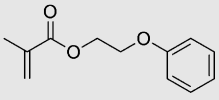	206.24
Poly(propylene glycol) acrylate (PPGA)	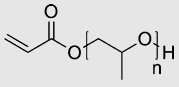	547
Poly(ethylene glycol) phenyl ether acrylate M_n 236 (PEGPEA236)	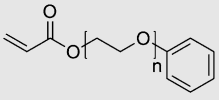	236
Poly(ethylene glycol) phenyl ether acrylate M_n 280 (PEGPEA280)	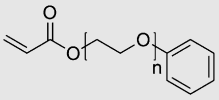	280
Poly(ethylene glycol) phenyl ether acrylate M_n 324 (PEGPEA324)	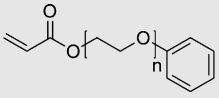	324
Benzyl acrylate (BZA)	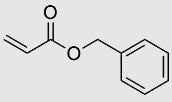	162.2

samples. For each material set in Tables S1–S4, each composition was tested at least twice ($n = 2$), one being from each batch. The testing apparatus was an MTS Insight 2 mechanical tester with a 100 N load cell. A thermal chamber (Thermcraft, Inc., model LBO-14-8-5.25-1X-J8249_1A) was used to isothermally test either at the glass transition temperature of each material or at another specified temperature. Once the chamber reached the set temperature, 10 min were given to insure equilibrium. A displacement rate of 1 mm/min was used, and the displacement was measured by the crosshead. Toughness was calculated by integrating the area under each stress–strain curve using the trapezoidal rule. The Kendall rank correlation coefficient (τ) was calculated to describe the relationship between select thermomechanical properties [35].

3. Results

The characteristic ratios from Table 1 were calculated using the method according to Wu [21] by the following equation:

$$C_\infty = (1/\varphi_0)^{2/3}\left[\left(\sum K_i + Bn_r\right)\Big/M_r\right]^{4/3}\left(M_v/\left\langle l_v^2\right\rangle\right) \quad (1)$$

$[(\sum K_i + Bn_r)/M_r]^{4/3}$ takes into account the intrinsic viscosity of the chain, where $\sum K_i$ sums the molar stiffness of each group. The molar stiffness constants for each group such as acrylic group or phenyl rings are detailed in the source [21]. B takes into account the tacticity of the chain, for example, for poly(methyl methacrylate) polymerized by free radical polymerization, $B \sim 4.12$. The CED for five mono-functional (meth)acrylates was calculated using the group contribution method outlined by Van Krevelen [26]. The molar volume (V_g) values used were for glassy amorphous polymers. The cohesive energy was calculated from the molar attraction values (F) using CED $= (F/V_g)^2$. Table 2 contains the calculated values. The monomers with aromatic sidegroups had higher CED values than the monomers with aliphatic side groups.

Materials were initially screened by creating a series of networks with either set multi-functional crosslinker or set mono-functional linear builder. The 16 networks in Table 3 were produced by polymerizing 10 mol% of PEGDMA550 and 90 mol% of each mono-functional monomer. The T_g and E_r were measured through DMA and showed a medium strength positive correlation as seen in Table S4. The T_g of the networks ranged from −29 to 112 °C, and the E_r ranged from 2.75 to 17.5 MPa. Generally, the T_g increased as the pendant length decreased or by the addition of an α-methyl group. The 16 networks in Table 4 were produced from 90 mol% tBA and 10 mol% of each crosslinker. The T_g and the E_r showed a medium strength positive correlation as seen in Table S5. The T_g ranged from −2 to 98 °C, and the E_r ranged from 6.48 to 129.5 MPa. As the functionality of the crosslinker increased, the E_r increased for equivalent mole fraction of crosslinking molecule. The increase in rubbery modulus is driven by the relative increase in mole fraction of crosslinking "bonds" for a crosslinker with higher functionality.

The 16 networks from Table 4 were tensile tested until failure to characterize their large strain mechanical properties including failure strain and toughness. The failure strain of each network is plotted against its corresponding E_r from DMA in Fig. 1. The failure strain ranged from less than 10% to over a 100%. The numbers 2–5, in the figure highlight the functionality of the crosslinkers. As expected, as the E_r of the network decreases the failure strain increases. For most crosslinkers, as the functionality of the crosslinker decreases, the rubbery modulus decreases, and the failure strain increases. Consistent with previous results, a significant effect of the crosslinker chemistry was not observed aside from property values governed by a change in crosslinking effectiveness measured through rubbery modulus.

DMA curves showing the change in crosslinker concentration for five targeted mono-functional (meth)acrylates are presented in Figs. S1–S5. The five linear (meth)acrylates were selected based on their differences in chemical structure and initial thermomechanical testing data. For all of these figures, the curve with the highest E_r is the pure PEGDMA550 curve. As the crosslinker concentration was decreased, the E_r decreased. As the concentration of crosslinker

Chart 2
Multi-functional monomers

Monomer	Structure	Molecular weight (g/mol)
Bisphenol A ethoxylate dimethacrylate M_n 1700 (BPA1700)	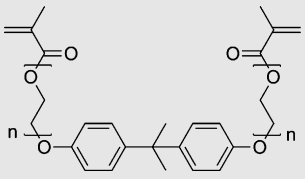	~1700
Bisphenol A ethoxylate dimethacrylate M_n 540 (BPA540)	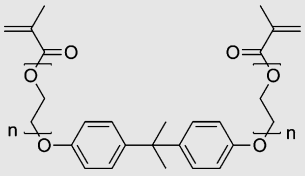	~540
Bisphenol A ethoxylate diacrylate M_n 688 (BPA688)	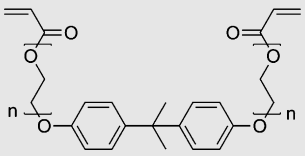	~688
Bisphenol A ethoxylate diacrylate M_n 512 (BPA512)	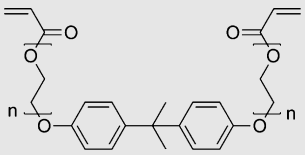	~512
Bisphenol A ethoxylate diacrylate M_n 468 (BPA468)	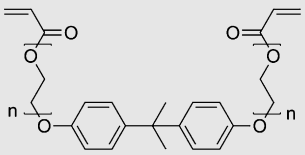	~468
Neopentyl glycol propoxylate diacrylate (NGPDA)	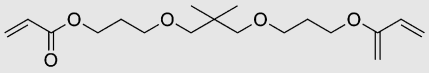	328
1,6-Hexanediol diacrylate (HEXDA)	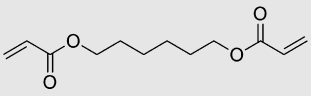	226
Poly(ethylene glycol) dimethacrylate M_n 550 (PEGDMA550)	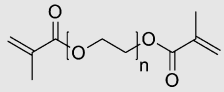	550
Pentaerythritol triacrylate (PETA)	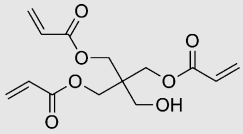	298
Trimethylolpropane ethoxylate triacrylate M_n 428 (TETA428)	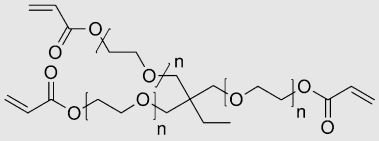	~428
Trimethylolpropane ethoxylate triacrylate M_n 604 (TETA604)	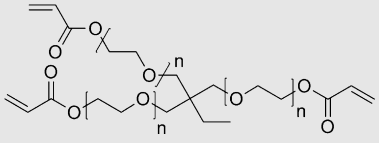	~604
Trimethylolpropane ethoxylate triacrylate M_n 912 (TETA912)	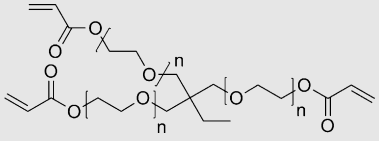	~912

(*continued on next page*)

Chart 2 (*continued*)

Monomer	Structure	Molecular weight (g/mol)
Trimethylolpropane propoxylate triacrylate (TPTA)	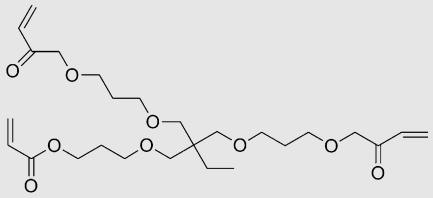	~644
Glycerol propoxylate triacrylate (GPTA)	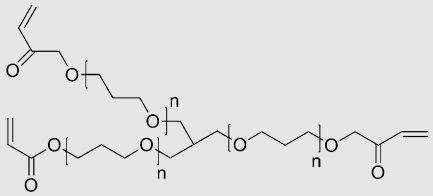	~428
Di(trimethylolpropane) tetraacrylate (DTTA)	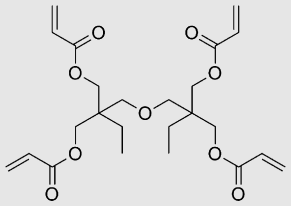	466
Dipentaerythritol penta/hexaacrylate (DPPHA)	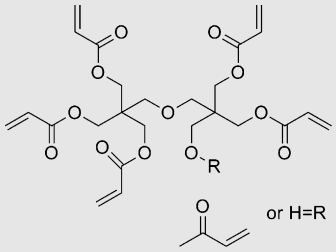	524

approaches zero, the E_r plateau disappears and E_r steadily decreases with increasing temperature. The T_g of each network increased as the concentration of crosslink E_r decreased. A non-linear trend is observed in Fig. 2, which shows the T_g of each composition from Tables S1 and S2. Fig. 3 displays the trend of the decreasing E_r as the crosslinker concentration decreased for the five systems. Systems start at the same point since each was originally composed of 100% PEGDMA550. Systems approach 0 MPa as the crosslinker concentration approaches 0%. The results in Figs. 2 and 3 demonstrate one of the known advantages of commercially available (meth)acrylate systems; using combination of various linear monomers and crosslinkers, one can independently tailor glass transition temperature and rubbery modulus. It is important to note that the PEGDMA550 crosslinker has equivalent impact on the five selected mono-functional monomers in terms of crosslinking effectiveness measured through rubbery modulus. The correlation coefficients between T_g and E_r for Figs. 2 and 3 is found in Table S5. These high correlation coefficients further support the decrease in T_g as E_r increases, since the T_g of the crosslinker was lower than the mono-functional monomers.

The networks in Tables S1 and S2 were tensile tested to large strains to understand the effect of structure on the large strain behavior of the networks. The failure strain of each composition from the tensile test was plotted against its respective E_r from DMA in Fig. 4. The results were plotted against E_r to eliminate any differences that may be a result of different "effective" crosslink density in the networks and thus isolate the effects of the linear monomer chemistry as a function of increasing crosslinker concentration. In addition, all tests in Fig. 4 were conducted at the T_g of the respective polymer (which differed significantly, vis-à-vis Fig. 2) to assure all networks were in an equivalent state of macromolecular motion. At E_r greater than 10 MPa (high crosslink density) the five systems had comparable failure strains for all compositions. At E_r lower than 10 MPa the network failure strains diverged significantly. As the E_r further decreased below 1 MPa, the networks did not display reliable rubbery plateaus, thus the data were excluded. The correlation coefficients between failure strain and E_r in Table S5 reveal the high inverse correlation between failure strain and E_r.

Table 1
Characteristic ratios of mono-functional monomers

Mono-functional monomer	C_∞
tBA	9.47
EEM	11.98
BZA	12.97
BMA	13.67
EGPEM	16.19

Table 2
CED of select mono-functional monomers

Monomer	CED (MPa)
BMA	396
BZA	424
EGPEM	401
EEM	358
tBA	332

Table 3
Thermo-mechanical properties of networks composed of 10 mol% PEGDMA550 with 90 mol% mono-functional (meth)acrylate

Mono-functional (meth)acrylate	T_g (°C)	E_r (MPa)
MMA	91.3	17.5
MA	23.5	11.75
BA	−15	7.3
tBA	40.5	10.7
tBMA	89.5	8.9
EEM	19.5	11.25
IMA	112	6.45
2EHM	20.5	7.7
BZA	23	10.51
IA	−23.5	6.5
BMA	68	9.4
EGPEM	40.5	12.75
PPGA	−29	2.75
PEGPEA236	10.5	6.1
PEGPEA280	−3.5	6.05
PEGPEA324	−9.5	4.45

To further support the results in Fig. 4, Fig. 5 displays representative stress–strain curves of the five systems with increasing rubbery moduli. For all five materials, as E_r decreases, the failure strain increases. The tBA, EEM, BZA, and EGPEM also show a decrease in strength as E_r decreases. Unlike the other systems, the BMA system does not show a steady decrease in strength as E_r decreases. The BMA has relatively higher failure strains and failure strengths as compared to the other materials at roughly equivalent rubbery modulus.

Fig. 6 displays the toughness, calculated as the area under stress–strain curves of the systems, as a function of the E_r. The systems have similar toughness at relatively higher E_r values, and the systems diverge at E_r values below 10 MPa. The tBA, EEM, BZA, and EGPEM systems have toughness values nearly a third of BMA. The point of divergence, the shape of the BMA stress–strain curves, and the increased toughness are points of interest to be further studied.

Networks composed of 2.5 mol% PEGDMA550-*co*-BMA or PEGDMA550-co-tBA from Table S3 were tensile tested across a range of temperatures, represented in Fig. 7. The objective of this testing was to verify that the relatively high toughness of the BMA material compared to tBA was not merely an artifact of a relative test temperature difference even though both materials were tested at their T_g defined as the peak in tan δ. The strain to failure in Fig. 7 is plotted at temperatures relative to each composition's respective T_g, $T - T_g$. A peak in failure strain is seen 15–20 °C before the T_g, then the curves level off when well into their respective rubbery region. The PEGDMA550-BMA curve reaches a higher peak and is broader than the PEGDMA550-tBA curve, highlighting the inherent toughness difference in the two materials that is not driven by a difference in effective crosslink density (measured through rubbery modulus) or temperature relative to T_g.

Mixtures of the various linear monomers were created with equivalent crosslinker concentration to determine how mechanical properties evolved from one network to another. From the ternary systems in Table S3, Fig. 8 shows the failure strain as a function of mol% BMA in three other linear monomers (all materials contain 2.5 mol% crosslinker). As the concentration of BMA increases, the failure strain increases. This trend is also seen in Fig. 9, which

Table 4
Thermo-mechanical properties of networks composed of 90 mol% tBA and 10 mol% multi-functional (meth)acrylate

Multi-functional (meth)acrylate	T_g (°C)	E_r (MPa)
BPA1700	−2.75	7.35
BPA540	70.5	8.15
BPA688	43.5	8.25
BPA512	64.5	9.0
BPA468	59.5	8.8
NGPDA	62.5	6.48
HEXDA	68.5	10.85
PEGDMA550	40.5	10.7
PETA	98	42.5
TETA428	83	25
TETA604	55	16.65
TETA912	24.5	15.95
TPTA	58	23
GPTA	69.5	15.5
DTTA	92	49.5
DPPHA	74	129.5

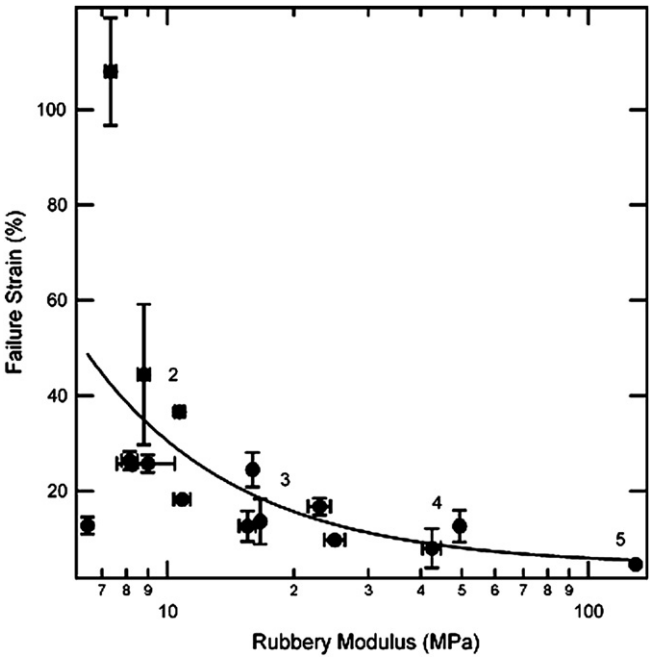

Fig. 1. Failure strain as a function of rubbery modulus for 16 networks composed of 90 mol% tBA and 10 mol% multi-functional (meth)acrylate. The numbers 2–5 give the functionality of the crosslinker.

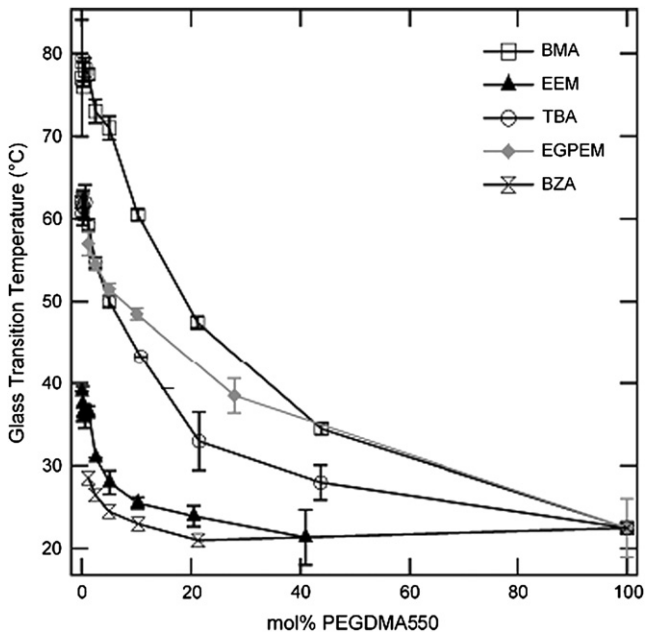

Fig. 2. Glass transition temperature as a function of mol% PEGDMA550 for five networks with varying mono-functional monomers.

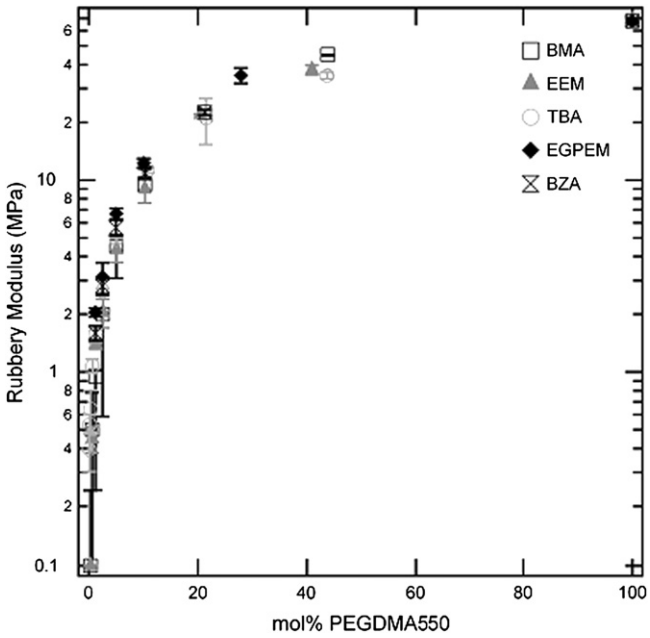

Fig. 3. Rubbery modulus as a function of mol% PEGDMA550 for five networks with varying mono-functional monomer.

describes the effect of increasing the concentration of BMA on the toughness of the networks.

4. Discussion

Polymer networks based on (meth)acrylate monomers have potential for a broad range of thermo-mechanical properties, making them strong candidates for shape memory materials. In order to understand the role of various components of these networks, mono-functional and multi-functional (meth)acrylates were used to synthesize a diverse set of polymer networks. Structure–property relationships were determined in these networks by studying their thermo-mechanical transitions and stress–strain response for systematically varied monomer functionalities, concentrations, and chemistries.

By holding crosslinker concentration constant, the effect of the mono-functional (meth)acrylate structure on the networks properties was determined. Chain backbone stiffness (capacity for conformational motion) and cohesive energy between chains are

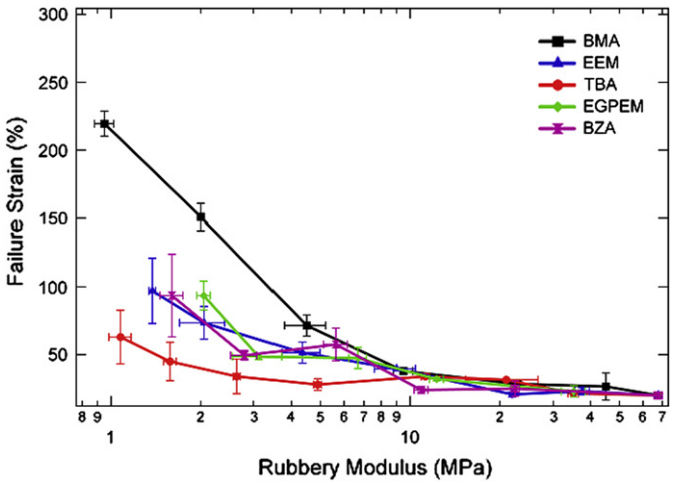

Fig. 4. Failure strain as a function of rubbery modulus for five networks of varying mono-functional monomer.

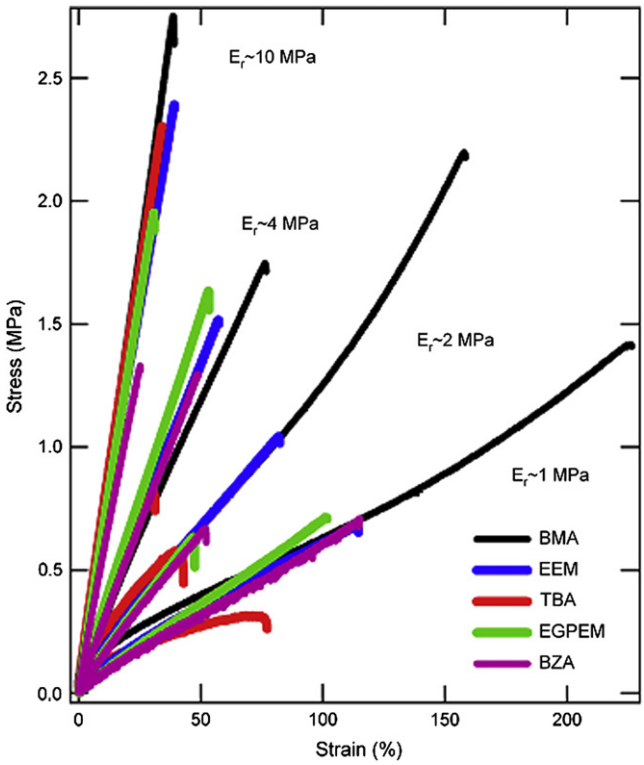

Fig. 5. Representative stress–strain curves of five networks for four rubbery moduli values.

the primary drivers for T_g, but crosslinking and other factors also participate [27]. The mono-functional (meth)acrylates with long sidegroups had the lowest T_g as may be expected based on the reduction of steric hindrance to conformational motion from the methylene and ester groups [36]. As the sidegroup length decreased and α-methyl side groups were added, the T_g increased due primarily to local steric hindrance of segmental conformational motion and increased cohesive energy between chains [37]. The

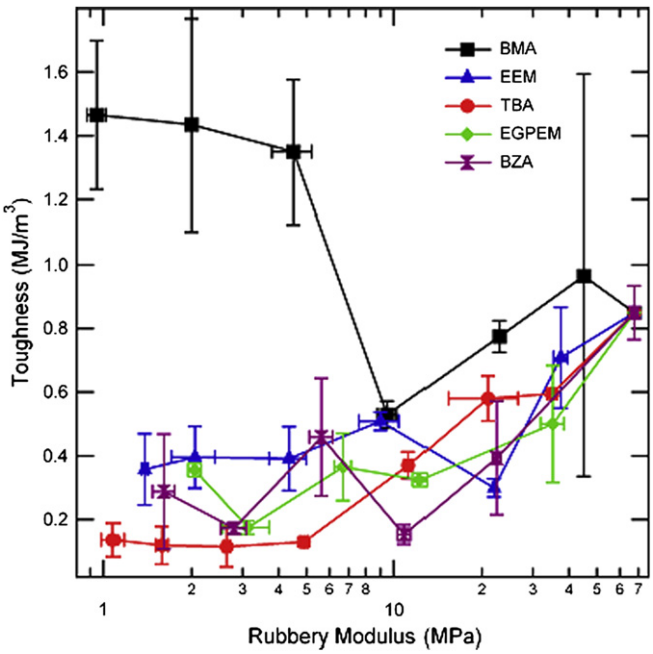

Fig. 6. Toughness as a function of rubbery modulus for five select networks of varying mono-functional (meth)acrylate.

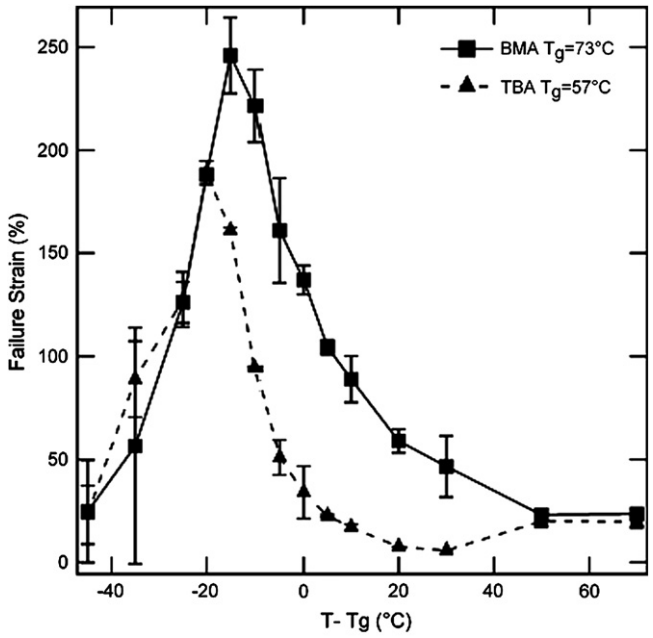

Fig. 7. Failure strain as a function of temperature relative to glass transition temperature for two networks at 2.5 mol% PEGDMA550.

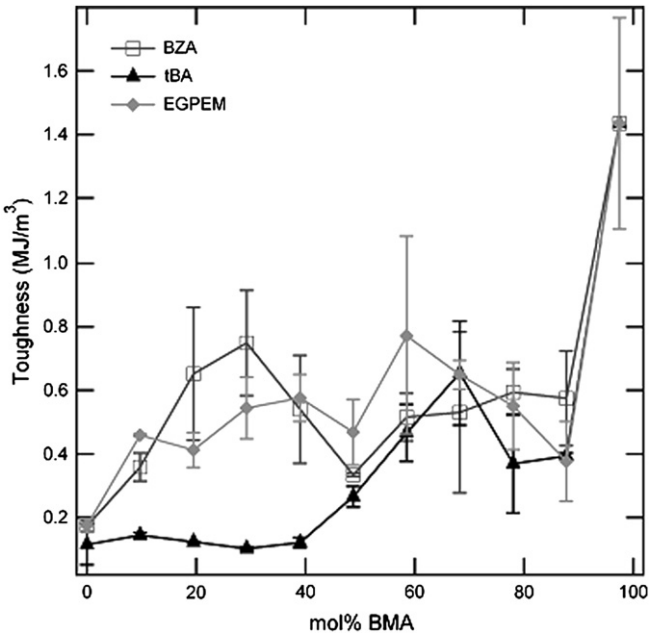

Fig. 9. Toughness as a function of mol% BMA for ternary networks with a fixed concentration of crosslinker.

effects are clear when combining the structures in Chart 1 with the T_g data from Table 3. Since these (meth)acrylates all have the same backbone, the sidegroup structure determines the T_g, and similar results in epoxies have demonstrated that the chemical structure of the amine alters T_g [38,39]. In summary, the combination of both α-methyl groups and short, rigid pendant groups on each side of the chain's backbone increases the T_g as can be seen in MMA and IMA.

In order to understand the effect of the crosslinker functionality on the networks, the mono-functional acrylate, tBA, was held constant and polymerized with various crosslinkers. The most identifiable trend was the relationship between the crosslinkers' functionality and E_r. It is known that as the crosslinkers' functionality increases, the network crosslink density increases, thus

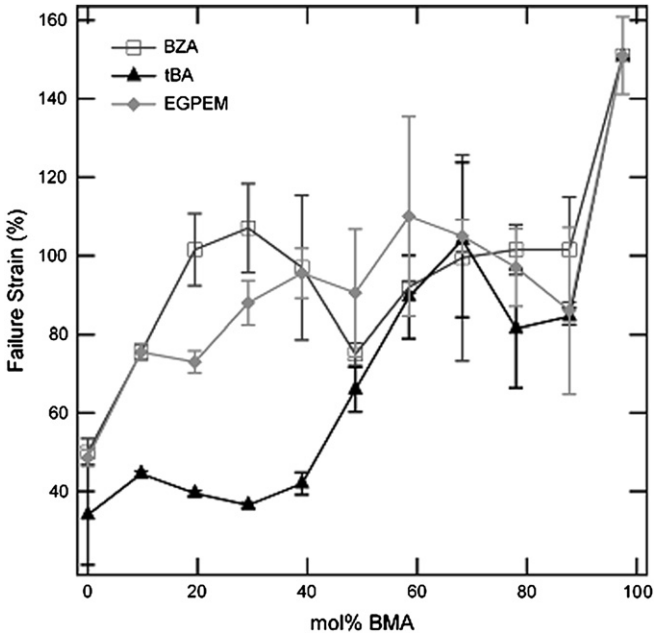

Fig. 8. Failure strain as a function of mol% BMA for ternary networks with a fixed concentration of crosslinker.

increasing E_r. This trend is clear in Fig. 1, where the failure strain is plotted against the E_r. Driven by different crosslinking effectiveness, the 16 networks trade-off failure strain and rubbery modulus. The majority of the networks with low E_r had higher failure strains than the high E_r networks. The materials with high E_r due to higher functionality were relatively brittle due to high crosslink density.

The above results highlight the capacity to readily adjust thermo-mechanical properties, a capacity that is central to an effective shape memory polymer. Aside from basic thermo-mechanical properties, it is important for some shape memory applications, and for deeper fundamental understanding, to examine large strain behavior of the networks. Prior work has examined the effect of varying crosslinker length and concentration on the large strain behavior of acrylate networks [18]. Here we focus on the reciprocal problem of varying mono-functional monomer for the same crosslinker added in varying concentrations. Five mono-functional monomers were chosen for differences in their transition temperatures, chemical structure, C_∞ and CED values.

In order to determine an appropriate testing temperature and provide a rough measure of effective crosslink density, T_g and E_r were measured for all five materials across all crosslink densities. Representative data for the systems are presented in Figs. S1–S5. As expected, the E_r decreases as the concentration of the crosslinker decreases in all networks. Since the selected crosslinker (PEGDMA550) has a relatively low T_g value when homopolymerized, the addition of it to all linear monomers serves to reduce T_g while increasing rubbery modulus. At 1 mol% crosslinker, the networks had reached their final T_g, thus further characterization was not continued for the BZA and EGPEM systems. Also, below a 1 mol% crosslinker concentration, the networks start to effectively transition to a thermoplastic, which is indicated by a loss of a rubbery modulus plateau. The breadth of the transition from the glassy to rubbery state decreases as the concentration of crosslinker decreases, as is expected because highly crosslinked systems have increased heterogeneity. The results here are consistent with previous studies where concentration of crosslinker was varied in acrylates [18].

The baseline thermo-mechanical experiments were necessary to assure that the selected test temperature is in the same

proximity of an individual composition's T_g and maintain equivalent states of molecular motion during large strain testing. A key finding of the tensile test was the existence of a divergence point, seen in Fig. 4 at a rubbery modulus of 10 MPa. Above 10 MPa, the crosslinking dominates the large strain mechanical properties of the network and a relatively brittle response is observed. It is important to note that although the mono-functional monomer has minimal impact on mechanical properties at these high crosslink densities, the mono-functional monomer choice will influence T_g of the network and consequently impact mechanical properties at a constant testing temperature. As E_r is decreased below 10 MPa, the large strain mechanical properties of the networks diverge and the capacity for strain and toughness depends on the choice of mono-functional monomer. Soon after entering the regime of mono-functional monomer sensitivity, the T_g of each network has reached close to a steady state value and thus there is no correlation between the absolute T_g of the network and the failure strain. This is evident in tBA and EGPEM having similar T_g's at low mol% PEGDMA550, but different failure strains at similar concentrations of PEGDMA550.

The stress–strain curves at representative rubbery moduli values were examined to understand the divergence of the failure strain. In general, the networks transition from brittle to ductile behavior as the E_r decreased is seen in Fig. 5. An inherent trade-off between strength and failure strain is evident in most networks with exception to the BMA network, which reached a high enough strain to exhibit non-linear strain-hardening even at reasonably high crosslink densities. This can be attributed to the reorientation of chains in the tensile direction [40]. As E_r decreases it becomes increasingly important to consider structural parameters of the mono-functional monomers. The strain to failure results do not correlate inversely with C_∞ values for the crosslinked networks as is common for thermoplastics. For example the C_∞ value for tBA is significantly lower than C_∞ for BMA although the latter has significantly higher failure strain at equivalent rubbery modulus. This observation implies that the capacity for network backbone chains to coil, as measured by C_∞, is incapable of predicting failure strain and toughness properties once these chains are moderately crosslinked. It seems that factors that toughen thermoplastics, such as coilability and high entanglement density are rendered less effective due to chemical crosslinking [18]. On the other hand, the CED may be used for relative comparison to determine if a material will strain farther through enhanced network toughness, as seen by combining Table 2 and Fig. 4. These results indicated that higher cohesive energy between chains, for equivalent crosslink density, serves to toughen the materials through increased resistance to fracture during large strain deformation. In other words, it appears that in the presence of moderate chemical crosslinking, strain to failure can be enhanced through improved toughness by increasing CED between chains.

Toughness was explicitly evaluated because of its importance during processing of shape memory polymers. Similar to failure strain, toughness diverges at 10 MPa, as seen in Fig. 6. Due to the strain-hardening that is observable in the stress strain behavior, BMA has the highest toughness below the divergence point while the other linear monomers have the same lower amount of toughness. The parameter C_∞ also breaks down when examining network toughness. For example, from Table 1 and Fig. 6, BZA, EGPEM, and EEM have different calculated C_∞, but exhibit similar levels of toughness.

In order to verify the inherently superior large strain mechanical properties of BMA networks, the test temperature should be eliminated as a factor influencing mechanical properties. To assure test temperature was not a factor in comparison of the networks, PEGDMA550-co-BMA and PEGDMA550-co-tBA, at the same mol% crosslinker (and the same rubbery modulus), were tested over a wide temperature range. These two materials were chosen because their failure strains and test temperatures differed by 100% and by more than 10 °C, respectively. Considering a sweep of test temperatures, the PEGDMA550-co-BMA network has inherent capacity for more deformation as observed in Fig. 7. It is interesting to note that the enhanced toughness of the BMA network only occurs at temperatures in the range of $T_g - 10$ °C to $T_g + 50$ °C. Thiol-ene/acrylate networks containing phenyl rings via Bisphenol A ethoxylate diacrylates have shown increased impact toughness near their T_g [41]. In the extreme temperature limits (glassy or rubbery) the failure strain of both materials is low and comparable. This result indicates that the toughening mechanism has an inherent viscous component that operates on distinct time and temperature scales.

To ascertain the influence of varying amounts of mono-functional monomers on mechanical properties, binary mixtures of mono-functional monomers with constant crosslinker concentration were formulated. With the BMA network as an upper bound of properties, the failure strain and toughness rise as BMA concentration increases, seen in Figs. 8 and 9. The BMA–BZA and BMA–EGPEM mixtures have higher failure strains and toughness values than the BMA–tBA mixtures, which may be due to the higher and more similar CED values of the monomers containing phenyl rings. The mechanical properties converge as the mol% BMA increases, near 70 mol% BMA. The properties of the BMA–BZA mixtures increase as the concentration of the α-methyl group increases, suggesting that the increased steric hindrance from the α-methyl group affects the mechanical properties. Likewise, the properties of the BMA–EGPEM mixtures increase as the phenyl ring is moved closer to the backbone by the subtraction of flexible ethylene glycol groups. Given these two trends, the transition from tBA to BMA is significant because both α-methyl and phenyl ring groups are being added to the network with increased BMA concentration. tBA lacks substantial deformation capacity because the failure strain and toughness do not increase until the majority of the network is BMA.

A method to theoretically predict (meth)acrylate network properties based upon the chemistry and structure has yet to be established. From this study, properties such as failure strain, toughness, T_g, and E_r can be tailored by varying the components of the network. The macromolecular parameter C_∞ is incapable of predicting failure strain and toughness in moderately crosslinked networks while CED can be used with some success in (meth)acrylate networks. New predictive parameters need to be developed or previous ones augmented to take into account key characteristics of network structure. In particular, the viscoelastic region is of great importance because shape memory polymers rely on approaching their T_g for actuation. In this region, both the monomer and network structure play a role in the large strain properties of the material as was demonstrated here [32].

5. Conclusion

The T_g of (meth)acrylate networks increases by adding α-methyl groups and moving bulky sidegroups close to the backbone. The crosslinking density rises as the functionality of crosslinkers increases, thus increasing the E_r and lowering failure strain. By varying chemistry and crosslinking density, a divergence point in network toughness is revealed, which delineates the crosslink-dominated region from the mono-functional monomer-dominated region. C_∞ was not an accurate predictor of network properties, particularly strain to failure and toughness at equivalent crosslink density. However, CED provided relative estimates of network strain to failure and toughness. (Meth)acrylates with phenyl rings close to the backbone proved to have superior large strain mechanical properties. This was confirmed across a range of temperatures and by ternary polymer systems. This study provides

insight into structure–mechanical property relationships in (meth)acrylates, but an encompassing theory for the prediction of large strain properties of networks of mono-functional and di-functional (meth)acrylates that incorporates chemical effects needs further study.

Acknowledgment

Financial support by Medshape Solutions' contributions to the School of Materials Science and Engineering is greatly acknowledged.

Appendix A. Supplementary data

Tables of mol% to wt% conversions for networks used. Correlation coefficients and figures showing representative DMA curves of five select networks. Supplementary data associated with this article can be found, in the online version, at doi:10.1016/j.polymer.2008.07.060.

References

[1] Maitland DJ, Metzger MF, Schumann D, Lee A, Wilson TS. Lasers in Surgery and Medicine 2002;30:1–11.
[2] Yakacki CM, Shandas R, Lanning C, Rech B, Eckstein A, Gall K. Biomaterials 2007;28:2255–63.
[3] Sharp AA, Panchawagh HV, Ortega A, Artale R, Richardson-Burns S, Finch DS, et al. Journal of Neural Engineering 2006;3:L23–30.
[4] Bowman CN, Peppas NA. Chemical Engineering Science 1992;47:1411–9.
[5] Kannurpatti AR, Anseth JW, Bowman CN. Polymer 1998;39:2507–13.
[6] Anseth KS, Wang CM, Bowman CN. Polymer 1994;35:3243–50.
[7] Anseth KS, Bowman CN. Chemical Engineering Science 1994;49:2207–17.
[8] Bowman CN, Carver AL, Kennett SN, Williams MM, Peppas NA. Polymer 1990;31:135–9.
[9] Anseth KS, Bowman CN, Peppas NA. Journal of Polymer Science, Part A: Polymer Chemistry 1994;32:139–47.
[10] Anseth KS, Kline LM, Walker TA, Anderson KJ, Bowman CN. Macromolecules 1995;28:2491–9.
[11] Moore JE. Photopolymerization of multifunctional acrylates and methacrylates. In: Labana SS, editor. Chemistry and properties of crosslinked polymers. New York: Academic Press; 1977.
[12] Goodner MD, Bowman CN. Chemical Engineering Science 2002;57:887–900.
[13] Lovell LG, Bowman CN. Polymer 2003;44:39–47.
[14] Yakacki CM, Shandas R, Safranski D, Ortega AM, Sassaman K, Gall K. Advanced Functional Materials 2008:18.
[15] Tobolsky AV, Katz D, Thach R, Schaffhauser R. Journal of Polymer Science 1962;62:S176–7.
[16] Gall K, Yakacki CM, Liu Y, Shandas R, Willett N, Anseth KS. Journal of Biomedical Materials Research Part A 2005;73A:339–48.
[17] Baer G, Wilson TS, Matthews DL, Maitland DJ. Journal of Applied Polymer Science 2007;103:3882–92.
[18] Ortega AM, Kasprzak S, Yakacki CM, Greenberg AR, Gall K. Journal of Applied Polymer Science 2008;110:1559–72.
[19] Raab M, Janacek J. International Journal of Polymeric Materials 1972;1:147–58.
[20] Flory PJ. Statistical mechanics of chain molecules. New York: Interscience; 1969.
[21] Wu S. Polymer Engineering and Science 1992;32:823–30.
[22] Wu S. Polymer International 1992;29:229–47.
[23] Wu S. Journal of Applied Polymer Science 1992;46:619–24.
[24] Xu Z, Hadjichristidis N, Fetters LJ, Mays JW. In: Structure/chain-flexibility relationships of polymers. Advances in Polymer Science, vol. 120. Berlin: Spring-Verlag; 1995.
[25] Ahmad H, Yaseen M. Polymer Engineering and Science 1979;19:858–63.
[26] Van Krevelen DW. Properties of polymers. Amsterdam: Elsevier; 1972.
[27] Bicerano J. Prediction of polymer properties. New York: Marcel Dekker; 1996.
[28] Bicerano J. Computational modeling of polymers. New York: Marcel Dekker; 1992.
[29] Zellers ET, Anna DH, Sulewski R, Wei X. Journal of Applied Polymer Science 1996;62:2081–96.
[30] Zellers ET, Anna DH, Sulewski R, Wei X. Journal of Applied Polymer Science 1996;62:2069–80.
[31] Bellenger V, Kaltenecker-Commercon J, Verdu J. Polymer 1997;38:4175–84.
[32] Pascault J, Sautereau H, Verdu J, Williams RJJ. Thermosetting polymers. New York: Marcel Dekker; 2002.
[33] Lee CJ. Polymer Engineering and Science 1987;27:1015–7.
[34] Lesser AJ, Calzia KJ. Journal of Polymer Science, Part B: Polymers Physics 2004;42:2050–6.
[35] Wessa P. Kendall tau rank correlation in free statistics software. Office for Research Development and Education; 2008.
[36] Gallardo A, San Roman J. Macromolecules 1993;26:3681–6.
[37] Seymour RB, Carraher CE. Structure–property relationships in polymers. New York: Plenum Press; 1984.
[38] Lesser AJ, Crawford E. Journal of Applied Polymer Science 1997;66:387–95.
[39] Crawford E, Lesser AJ. Journal of Polymer Science, Part B: Polymers Physics 1998;36:1371–82.
[40] Ward IM. Mechanical properties of solid polymers. New York: Wiley-Interscience; 1971.
[41] Senyurt AF, Wei H, Hoyle CE, Piland SG, Gould TE. Macromolecules 2007;40(14):4901–9.